H^{∞} Robust Differential Control for Electromagnetic Suspension Beam

Peipei Wang [a], Changsheng Zhu [b]

[a] College of Electrical Engineering, Zhejiang University, Hangzhou 310027, China, E-mail: 21710195@zju.edu.cn
[b] College of Electrical Engineering, Zhejiang University, Hangzhou 310027, China

***Abstract*—To stabilize the magnetic levitation beam, a robust control model is established and H_∞ robust controller is designed based on the hybrid sensitivity H_∞ theory. Dynamic and state characteristics are analyzed using numerical simulation and experiment. The results show that the designed controller can realize the stable suspension, which further validates the effectiveness of the proposed approach.**

I. INTRODUCTION

In the research of magnetic levitation systems, the single degree-of-freedom(DOF) magnetic levitation system has a simple structure and is easy to implement, therefore, studying a single DOF magnetic levitation system is an effective method for further studying the magnetic levitation technology.

In this paper, a control system for an open-loop unstable single DOF magnetic levitation beam is designed based on the hybrid sensitivity H_∞ theory. The simulation analysis and experiments are carried out to verify the effectiveness of control system. The results show that the designed control system has good dynamic performance and steady state performance.

II. SYSTEM STRUCTURE AND MODELING

A. Magnetic Levitation Beam System

Structure of magnetic levitation beam system is shown in Fig.1, which is consisted of controller, power amplifier, Hall displacement sensor, electromagnet, and a beam which is supported in the middle by a tapered bracket. It is a typical magnetic levitation system with only one degree of freedom.

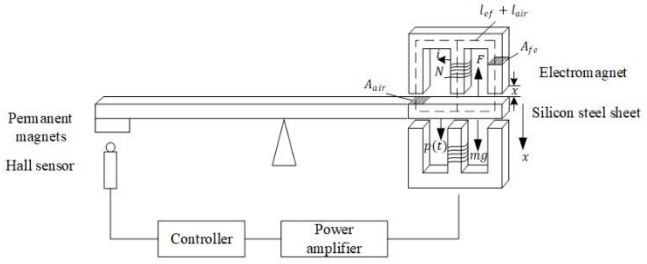

Fig. 1 Structure of magnetic levitation beam

However, the magnitude of the electromagnetic force between the electromagnet and the beam is inversely proportional to the air gap between them. When the current in the coil is constant, the larger the air gap between the electromagnet and the beam, the smaller the electromagnetic force will be. Therefore, the magnetic levitation system is an inherently open-loop unstable system. To achieve a stable suspension of the system, a closed-loop feedback control must be implemented and a controller is necessary.

The purpose of the controller is to control the coil current to keep the beam levitated in stable position. In this paper, the coil current is controlled by PSoC. This current applied to the coil produces the magnetic force on the beam. If the load is increased, the sensor senses the displacement and delivers signal to PSoC. The PSoC receives the signal and changers the current supplied to the corresponding coil. Thus, the magnetic force is increased and the beam is levitated stably. If the load is decreased vice-versa activity is occurred.

Hall effect sensor and permanent magnet are combined to detect the beam position, due to cheap and easily purchased in a local electronics store. The permanent magnet is fixed at the right end of the beam, and the Hall sensor is placed underneath. When the position of the beam varies, the output voltage of the Hall sensor varies too, and it is proportional to the position of the beam. When the beam has displaced from its levitated position, the sensor provides a signal to the control unit. Then the control unit regulates the supply of current to coil according to the information provided by sensor to bring back the disturbed beam to its stable position.

To facilitate the coil winding, E shape core is selected for the design of electromagnet. And Laminated iron core was chosen to make the electromagnet because it has good magnetic permeability and hysteresis characteristics and its operating temperature range is high.

B. Mathematical Model

Since the magnetic circuit of the "E" shape electromagnet is symmetrical, the “E” shape electromagnet can be equivalent to a "U" shape electromagnet in the modelling. We use "U" shape electromagnet for the following analyses.

It is assumed that the magnetic field is uniform in the air gap, the magnetic flux passes through the iron core completely, the influence of hysteresis is ignored and the core is considered to be unsaturated.

First, we define the following symbols: l_{fe} is the average length of the magnetic circuit of the core (m), x is the air gap between the electromagnet and the beam (m), A_{fe} is the cross-sectional area of the core (m^2), A_{air} is the cross-sectional area of the air gap between the electromagnet and the beam (m^2), H_{fe} is the strength of the magnetic field of the core (A/m), H_{air} is the strength of the magnetic field in the air gap (A/m), μ_r is the relative permeability of the core (H/m), μ_0 is the air permeability (H/m), N is the number of turns of the coil winding, B_{fe} is the magnetic induction of the core (T), B_{air} is

the magnetic induction in the air gap (T), $\emptyset_{fe}$ is the magnetic flux of the core (Wb), $\emptyset_{air}$ is the magnetic flux in the air gap (Wb).

Fig 2 shows the simplified model of the electromagnet.

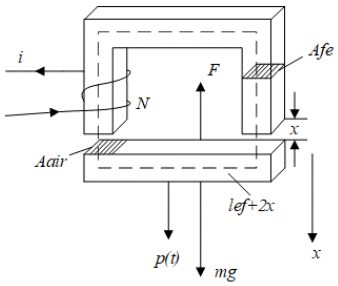

Fig. 2 The simplified model of the electromagnet

According to Maxwell's equations, the electromagnetic force of the electromagnet to the beam is as

$$F = \frac{{B_{fe}}^2 A_{fe}}{\mu_0} \tag{1}$$

According to Ampere loop theorem, the equation of the magnetic circuit in Fig.2 is

$$NI = \oint Hdl = l_{fe}H_{fe} + 2xH_{air} \tag{2}$$

and

$$H = \frac{B}{\mu} = \frac{\emptyset}{\mu A} \tag{3}$$

Assuming that the magnetic field is uniform, equation (3) will be

$$Ni = l_{fe}\frac{B_{fe}}{\mu_0\mu_r} + 2x\frac{B_{air}}{\mu_0} = l_{fe}\frac{\emptyset_{fe}}{\mu_r\mu_0 A_{fe}} + 2x\frac{\emptyset_{air}}{\mu_0 A_{air}} \tag{4}$$

Since we do not consider the magnetic flux leakage, which means all the magnetic flux passes through the iron core, and the A_{fe} of the entire loop is constant, so

$$H = \frac{B}{\mu} = \frac{\emptyset}{\mu A} \tag{5}$$

where

$$\emptyset_{fe} = B_{fe}A_{fe} \tag{6}$$

$$\emptyset_{air} = B_{air}A_{air} \tag{7}$$

The cross-sectional area of the core is equal to the area of the air gap, i.e.,

$$A_{fe} = A_{air} = A \tag{8}$$

From equations (7) and (8), we have

$$B_{fe} = B_{air} = B \tag{9}$$

According to equations (5), (8) and (9), equation (4) is transformed as

$$B = \frac{\emptyset}{A} = \frac{Ni}{\frac{l_{fe}}{\mu_r\mu_0} + \frac{2x}{\mu_0}} \tag{10}$$

Because $\mu r \gg 1$, equation (10) can be approximated as

$$B = \frac{\mu_0 Ni}{2x} \tag{11}$$

So, equation (1) will be

$$F = \frac{\mu_0 N^2 i^2 A}{4x^2} = k\frac{i^2}{x^2} \tag{12}$$

$$k = \frac{\mu_0 N^2 A}{4} \tag{13}$$

From equation (12), we can see that when structural parameters of the system are fixed, i.e., when the air gap area A and the number of turns of the coil winding N are constant, the electromagnetic force F is proportional to the square of the current i and it is inversely proportional to the square of the air gap x, i.e., the magnetic force is nonlinear. Therefore, in order to facilitate the design of the electromagnetic suspension beam system, linearization about the electromagnetic force is necessary.

When the system operates near the equilibrium point, it can be regarded as a linear process. According to Taylor's formula in the neighborhood of the equilibrium point $(i = i_0, x = x_0)$, equation (12) can be expressed as

$$F(i,x) \approx F(i_0,x_0) + \frac{\partial F(i_0,x_0)}{\partial i}(i - i_0) + \frac{\partial F(i_0,x_0)}{\partial x}(x - x_0) \tag{14}$$

Take its partial with respect to x and i,

$$\frac{\partial F(i,x)}{\partial x} = -2k\frac{i^2}{x^3} \tag{15}$$

$$\frac{\partial F(i,x)}{\partial i} = 2k\frac{i}{x^2} \tag{16}$$

Plugging equation (12) into equations (15) and (16), we can get

$$\begin{cases} \frac{\partial F(i_0,x_0)}{\partial x} = -2k\frac{{i_0}^2}{{x_0}^3} = -\frac{\mu_0 N^2 A {i_0}^2}{2x_0^3} = k_x \\ \frac{\partial F(i_0,x_0)}{\partial i} = 2k\frac{i_0}{{x_0}^2} = \frac{\mu_0 N^2 A i_0}{2x_0^2} = k_i \end{cases} \tag{17}$$

k_x and k_i represent the displacement stiffness and the current stiffness of the system, respectively. k_x is negative, i.e., when the displacement decreases, the electromagnetic force increases; when the displacement increases, the electromagnetic force decreases. Once the structural parameters of the system are fixed, k_x and k_i are constants.

Substituting equation (17) into equation (14), the linearized approximation of the electromagnetic force when the system works near the equilibrium point $(i = i_0, x = x_0)$ will be

$$F(i,x) \approx F(i_0,x_0) + k_i(i - i_0) + k_x(x - x_0) \tag{18}$$

When the system works near the equilibrium point, the angle of rotation of the beam is very small. So, the motion of the levitated beam can be considered to be translation. Taking the direction in which x increases as the positive direction, the equation of motion of the magnetic levitation beam system is,

$$m\frac{d^2x}{dt^2} = mg - F(i,x) + p(t) \tag{19}$$

where $p(t)$ is the external disturbance force in the x direction, which is a function of time t, $F(i,x)$ is the electromagnetic force generated by the electromagnet, which is a function of the air gap x and current i. Mg is the equivalent gravity of the levitated beam in the equilibrium position.

Since $F(i_0,x_0)$ is the electromagnetic force when the system works at the equilibrium point, and $F(i_0,x_0) = mg$, the equation of motion of the magnetic levitation beam will be

$$m\frac{d^2x}{dt^2} + k_i i + k_x x = p(t) \tag{20}$$

Laplace transformation of equation (20) is

$$ms^2X(s) + k_i I(s) + k_x X(s) = P(s) \tag{21}$$

When the external disturbance force disappears, the transfer function of the current i and the air gap x will be

$$\frac{X(s)}{I(s)} = \frac{-k_i}{ms^2 + k_x} \tag{22}$$

According to equation (22), the open-loop poles of the system are $s = \pm\sqrt{-k_x/m}$. One of the poles falls on the right half-plane of S plane, which means the open-loop magnetic levitation beam system is unstable. Therefore, a closed-loop control is necessary.

Take the air gap x and the velocity $\dot{x}$ as the state variables of the system, i.e., $\boldsymbol{X} = [x \quad \dot{x}]^T$, the current i as the input of the system, and the air gap x as the output of the system. The state space mathematical model of the system is

$$\begin{cases} \dot{X} = \begin{bmatrix} 0 & 1 \\ -\frac{k_x}{m} & 0 \end{bmatrix} X + \begin{bmatrix} 0 \\ -\frac{k_i}{m} \end{bmatrix} i \\ y = [1 \quad 0]X \end{cases} \tag{23}$$

The magnetic flux in core is

$$\emptyset = BA = \frac{\mu_0 NiA}{2x} \tag{24}$$

The flux linkage is

$$\varphi = N\emptyset = \frac{\mu_0 N^2 iA}{2x} = Li \tag{25}$$

From equation (25), we can obtain the inductance of the electromagnet as

$$L = \frac{\mu_0 N^2 A}{2x} \tag{26}$$

According to equation (26), the electromagnetic voltage is

$$U = \frac{d(Li)}{dt} + Ri = \left(\frac{\mu_0 N^2 A}{2x}\right) \cdot \frac{di}{dt} - \frac{\mu_0 N^2 Ai}{2x^2} \cdot \frac{dx}{dt} + Ri \tag{27}$$

where R is the coil resistance.

III. DESIGN OF ROBUST CONTROLLER

Compared with the traditional control method, the robust H_∞ control does not depend on the accurate mathematical model of the system and can achieve robust performance and stability in the presence of bounded modelling errors.

A. *The hybrid sensitivity H_∞ control*

The block diagram of H_∞ standard control is shown in Fig.3. w is the external input, including the reference input, interference and noise. z is the generalized control error, also known as the evaluation signal, including tracking error, adjustment error and actuator output. u is the controller output. y is the observation output, for instance, the sensor output. $G(s)$ is the generalized controlled object, including the actual controlled object and weighting functions. $K(s)$ is the controller. It is noteworthy that the generalized controlled object is not equivalent to the actual controlled object.

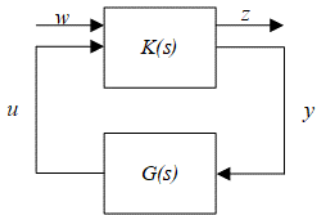

Fig. 3 H_∞ standard control

Dividing $G(s)$ into four blocks according to the dimensions of w, z, y, and u, we have

$$\mathrm{G(s)} = \begin{bmatrix} G_{11}(s) & G_{12}(s) \\ G_{21}(s) & G_{22}(s) \end{bmatrix} \tag{28}$$

The state space model of the system can be represented as

$$\begin{cases} z = G_{11}w + G_{12}u \\ y = G_{21}w + G_{22}u \\ u = ky \end{cases} \tag{29}$$

The relationship between z and w will be

$$\mathrm{z} = (G_{11} + G_{12}\mathrm{K}(\mathrm{I} - G_{22}\mathrm{K})^{-1}G_{21})\mathrm{w} \tag{30}$$

where $(\mathrm{I} - G_{22}\mathrm{K})^{-1}$ is an invertible real rational matrix.

Then we can get the closed loop transfer function from w to z as

$$\mathrm{P(s)} = \frac{Z(s)}{W(s)} = G_{11} + G_{12}\mathrm{K}(\mathrm{I} - G_{22}\mathrm{K})^{-1}G_{21} \tag{31}$$

The H_∞ standard problem is to design a real and rational feedback controller $K(s)$ for a given generalized controlled object $G(s)$, and to make the closed-loop system be stable with the H_∞ of the transfer function matrix $P(s)$ being minimal.

The hybrid sensitivity H_∞ control is a type of robust control that selects reasonable weighting functions to achieve the desired performance of the closed-loop system.

The block diagram of hybrid sensitivity H_∞ control is shown in Fig.4, where r is the reference input, e is the tracking error, u is the controller output, z_1, z_2, z_3 is the evaluation signal, y is the system output, d is the interference input, n is the measurement noise, and w_1, w_2, w_3 are the sensitivity weighting function, the linear weighting function, and the complementary sensitivity weighting function respectively.

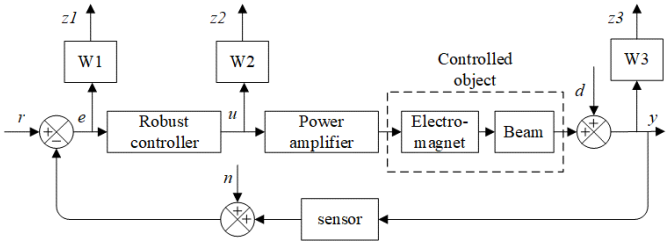

Fig. 4 The block diagram of the hybrid sensitivity H_∞ control

The transfer functions from r to e, r to u, r to y are respectively

$$\begin{cases} S = \frac{E(s)}{R(s)} = (1 + GK)^{-1} \\ R = \frac{U(s)}{R(s)} = K(1 + GK)^{-1} \\ T = \frac{Y(s)}{R(s)} = GK(1 + GK)^{-1} \end{cases} \tag{32}$$

S is the sensitivity function, T is complementary sensitivity function, and $S + T = I$.

$$\mathrm{z} = \begin{bmatrix} z_1 \\ z_2 \\ z_3 \end{bmatrix} \tag{33}$$

The transfer function from the reference input r to the evaluation signal z is

$$\mathrm{P} = \begin{bmatrix} W_1 & S \\ W_2 & R \\ W_3 & T \end{bmatrix} \tag{34}$$

To design a hybrid sensitivity H_∞ controller is to design a controller $K(s)$ to stabilize the system, and to minimize the norm of the transfer function matrix $P(s)$, i.e.,

$$\min\|P\|_\infty = min \begin{bmatrix} W_1 & S \\ W_2 & R \\ W_3 & T \end{bmatrix} = \gamma,\ \gamma \gg \gamma_0 \tag{35}$$

B. Choice of Weighting Functions

$W_1(s)$ is the weighting function of the sensitivity function S of the system, which reflects the relationship between the tracking error e and the reference input r, and also reflects the relationship between the system output y and the interference input d. Therefore, the choice of $W_1(s)$ is important, as it's related to the ability of the system to suppress the external disturbance. Since the actual disturbance usually occurs in the low-frequency region, in order to suppress the disturbance, the low-pass $W_1(s) = 100/(s + 0.01)$ is selected.

$W_2(s)$ is the weighting function of the transfer function R from the system's reference input to the control output. $W_2(s)$ is designed to constraint the output of the controller, and prevent excessive damage caused by excessive control or saturation of the controller. Meanwhile, in order to simplify the controller design without increasing the order of controllers, $W_2(s)$ is selected as a real constant, i.e., $W_2(s) = 10^{-5}$.

$W_3(s)$ is the weighting function of the complementary sensitivity function T. $W_3(s)$ is related to the dynamics of unmodeled components and uncertainty of the system parameters. Because the disturbance caused by the uncertain of the system model is mainly concentrated in the high frequency region, in order to maintain the robustness of the system and to suppress the disturbance with high frequency, high-pass $W_3(s) = (0.001s^2 + s)/1000$ is selected.

The Bode diagrams of the $W_1(s)$ and $W_3(s)$ are shown in Fig.5 and Fig.6. It can be seen that the sensitivity weighting function $W_1(s)$ has a low-pass characteristic and the complementary sensitivity weighting function $W_3(s)$ has a high-pass characteristic, and the cut-off frequency of $W_3(s)$ is greater than the cut-off frequency of $W_1(s)$, which meets the selection requirements of weighting functions.

The discrete pulse transfer function of the corresponding robust controller for the above weighting function is

$$G_c(s) = \frac{-11.91z^3+10.76z^2+11.88z-10.79}{z^3-1.754z^2+0.9389z-0.1846} \tag{36}$$

Using the robust control toolbox of MATLAB, the discrete pulse transfer function of the digital robust controller can be converted to input-output forms.

$$\begin{aligned} u(k) = {} & -11.91e(k) + 10.76e(k-1) + 11.88e(k-2) \\ & -10.79e(k-3) + 1.754u(k-1) \\ & -0.9389u(k-2) + 0.1846u(k-3) \end{aligned} \tag{37}$$

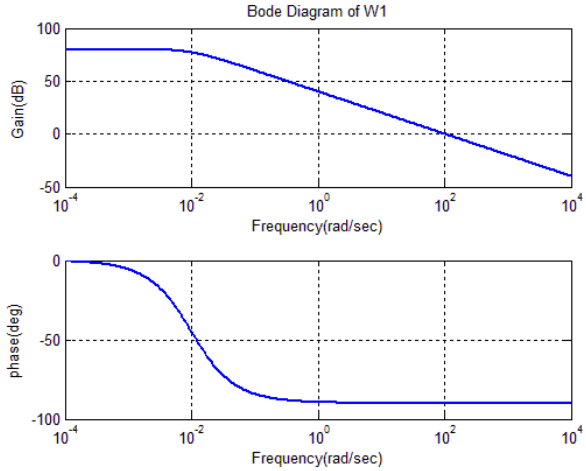

Fig. 5 Bode Diagram of $W_1(s)$

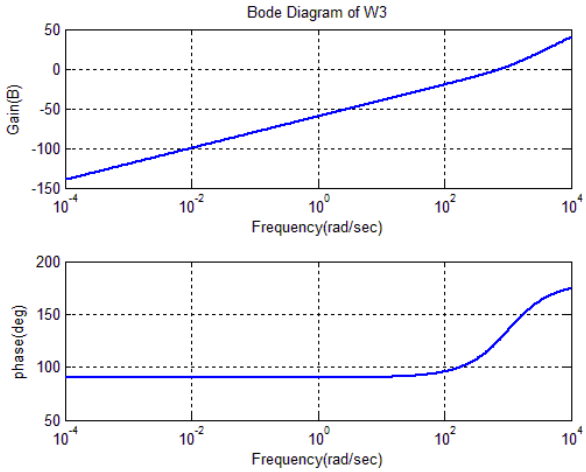

Fig. 6 Bode Diagram of $W_3(s)$

IV. Simulation and Experimental Results

Fig.7 shows the simulation results of the magnetic levitation beam system with the designed robust controller. The three curves are corresponded to the mass of beam of 20 g, 40 g and 60 g and a disturbance is applied at 0.2 second. From the results, we can see that after 0.1 seconds the system is stable from initial operation point which is about 25 mm of the beam position. And the robust controller can stabilize the system under all the three circumstances. After a disturbance is applied to the system at 0.2 second, the system recovers stability quickly within 0.1 seconds.

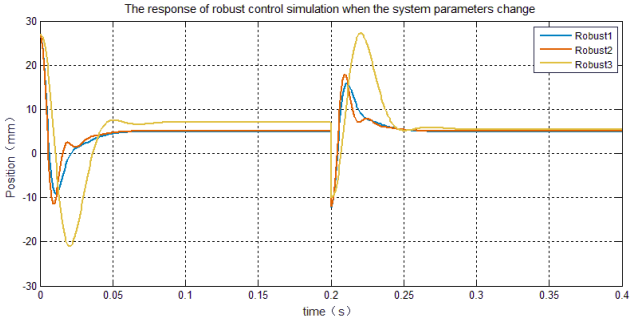

Fig. 7 Simulation results of the response in robust control when the mass of beam change

Fig.8 shows the simulation results of the robust control system when the gain of sensor is 250, and Fig.9 shows the simulation results of the robust control system when the gain of sensor is 500. In both cases, the designed robust controller can keep the system stable, while it takes longer to stabilize the system when the gain of sensor is 250.

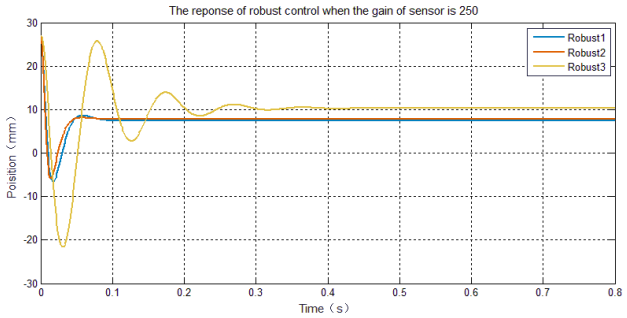

Fig. 8 Simulation results of the response in robust control when the gain of sensor is 250

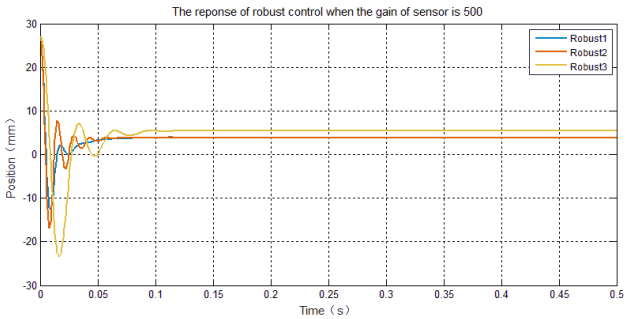

Fig. 9 Simulation results of the response in robust control when the gain of sensor is 500

Fig.10 shows the magnetic levitation beam test platform with the designed robust controller. Fig.11 shows the experimental results with a large disturbance applied to the beam after the beam is levitated stably.

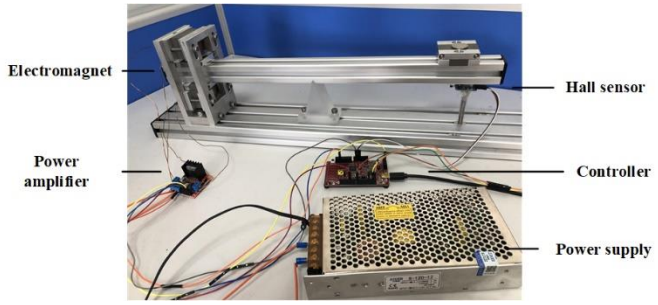

Fig. 10 Experimental platform

The experiment results show that the designed robust controller can make the maglev system suspend stably in a certain equilibrium position with good static performance. And the system can respond quickly when it is disturbed, indicating strong anti-interference ability. When using PID controller, the system can only tolerate relatively small disturbance. Once a large disturbance is applied, the beam will fall down. While using the robust controller, the system can tolerate larger disturbance, and still maintain stability. In the experiment, we put a heavy object on the right end of the beam, which is to change the weight of the beam, and found that the beam would still achieve stability, which verifies the simulation results that the robust control can suppress disturbances effectively and the system is robust in the case of parameter perturbation.

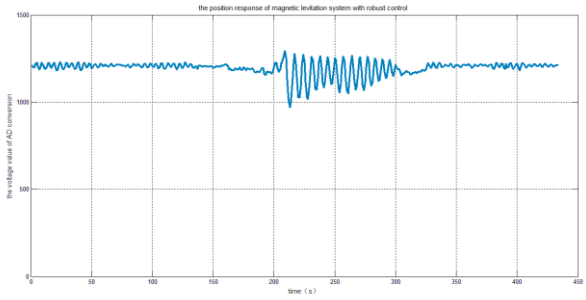

Fig. 11 Experimental result of the response in robust control when adding large disturbances

V. CONCLUSIONS

In this paper, the linear mathematical model of a single DOF magnetic levitation beam system is established. Taking into account the limitations of traditional control methods, the presence of uncertainties such as errors in the modeling process, external disturbances and sensor noise, the hybrid sensitivity H_∞ control method is adopted to design the hybrid sensitivity robust controller. The simulation and experimental results show that the closed-loop system has good dynamic performance and steady state performance and it is robust stable in the case of external disturbance and system parameter changing.

VI. ACKNOWLEDGE

This work was supported in part by the National Natural Science Foundation of China under Grant 11632015 and Grant 51477155, and the Project of Collaborative Innovation Center of Advanced Aero-engine.

REFERENCES

[1] Yang Z J, Miyazaki K, Kanae S, et al. “Robust position control of a magnetic levitation system via dynamic surface control technique,” *IEEE Transactions on Industrial Electronics*, pp. 26-34, 2004.

[2] Hasirci U, Balikci A, Zabar Z, et al. “A novel magnetic-levitation system: design, implementation, and nonlinear control,” *IEEE Transactions on Plasma Science*, pp. 492-497, 2011.

[3] Huang H, Du H, Li W. “Stability enhancement of magnetic levitation ball system with two controlled electomagnets,” *IEEE power Engineering Conference*, pp. 1-6, 2015.

[4] Shawki N, Alam S, Gupta A K S. “Design and implementation of a magnetic levitation system using phase lead compensation technique” *IEEE International Forum on Strategic Technology*, pp. 294-29 2014.